

HELICOPTER ROTOR FREE WAKE CALCULATIONS USING A NEW RELAXATION TECHNIQUE

G. H. Xu

Research Institute of Helicopter Technology, Nanjing University of Aeronautics & Astronautics,
Nanjing 210016, P. R. China

S. J. Newman

Department of Aeronautics and Astronautics, University of Southampton,
Southampton SO17 1BJ, UK

Abstract

A new algorithm for improving the convergence characteristics of rotor free-wake calculations in hover and low-speed forward flight is presented in this paper. The algorithm is a periodic relaxation iteration approach which incorporates the relaxation of wake collocation points with the average of velocities according to the finite-difference scheme. Based on the algorithm, a free-wake analytical method for rotors has been developed. In order to validate the method, the induced velocity distributions and tip vortex displacements of rotors are calculated and compared with the available experimental data. The computational comparisons between the present relaxation method and a time-stepping method for a chosen advance ratio are also performed and the conclusion that the two different types of wake solution methods can give the unique convergence result is obtained. The numerical characteristics of the present method have been investigated and its robustness and improved computational efficiency are demonstrated. Finally, this method is applied to examine the wake structure of a helicopter rotor from hover through low-speed forward flight and the transition of the wake geometry is analysed.

1. Introduction

The accurate prediction of the rotor flow field is fundamental to the design of next-generation helicopters with improved aerodynamics and dynamics. The dominant feature of the rotor flow field is the strong vortical wake structure trailed from the blades. Unlike the fixed-wing aircraft, the rotor wake vortices of helicopters move downstream in close proximity to the rotor, which significantly influences the variation of the local flow velocity

and loading of the blades. Therefore, the accurate prediction of the rotor wake is essential to the calculation of the rotor flow field. Rotor wake modelling has been an important research area in rotor/helicopter aerodynamics (e.g., Refs.1-7). There exist rigid, prescribed and free wake models, but free-wake modelling, which allows the wake vorticity to convect in free motion, is considered to be the most accurate and physically correct approach to rotor designs. There are two main concerns in the free wake calculations that are its numerical stability and computational efficiency. Although more powerful computers are available nowadays, there is still a strong need to reduce the computation time for the free-wake computation in order for routine design analysis.

It has been known that the free wake calculations using the conventional time-stepping method will encounter numerical instabilities or convergence difficulties in hover and low-speed forward flight. This is the significant regime for the rotor/airframe interactional problem and the critical transition regime from the viewpoint of stability and control and vibration. Refs. 8, 9 and 10 describe the problems in some details. One conjecture is that the poor stability may be partially due to the inherent physical instability in the rotor wake vortex system, however, more recent studies argue that the problem mainly results from the numerical method used in the solutions. In essence, the previous time-stepping method is a type of explicit one, which extrapolates the wake position to next time step, and one well-known problem with the explicit scheme is its poor numerical stability. The numerical instability will lead to the severe divergence of the wake solution if left unconstrained. In order to suppress the instability, some of the previous research tried to

introduce a numerical damping such as an artificially large tip vortex core to the time-stepping solutions. Unfortunately, such a damping may impose a force on the force-free wake and thus the results may not be used reliably.

Considerable progress has been made in the studies on improving the convergence of the free wake computation over recent years. In the hover wake analysis, Rosen and Graber introduced a relaxation factor to free-wake calculations (Ref. 11), which helped improve some of the numerical instability. Quakenbush et al also incorporated an influence coefficient relaxation technique in a comprehensive hover performance code (Ref. 12). In the forward-flight analysis, Miller and Bliss presented a new periodic inversion approach (Ref. 13). The centre feature of the approach is to define the wake collocation points in a non-Lagrangian sense and to employ the periodic boundary condition. Their work showed the important potential of the relaxation methods in improving the forward-flight and hover wake calculations. However, the approach requires solving a large set of coupled algebraic equations, which is too computationally expensive for the use in routine rotor analyses. Crouse and Leishman (Ref. 14) gave a predictor-corrector approach using the three-point finite difference scheme to the governing differential equation of wake. On the basis of Ref. 14, Bagai and Leishman (Ref. 15) presented a pseudo-implicit predictor-corrector (PIPC) approach using a five-point difference technique. The PIPC approach was also extended to the coaxial rotor wake analysis (Ref. 16) and the manoeuvring rotor wake analysis (Ref. 17), but the problem of computational efficiency still remains. Since the PIPC approach is a two-step scheme, it requires solving the induced velocity field twice for every iterative rotor revolution and, as such, it requires twice the computation time of time-stepping methods. It has been well known that the computation of induced velocities on all the wake collocation points is a dominant part in the wake computation time. The problem of computational efficiency will become more important with the increase of the number of vortex filaments chosen and the reduction of time steps used, especially in the computations of the unsteady rotor/fuselage interaction, the rotor/tail rotor interaction and the blade-vortex interaction

where the time step is required to be discretized more finely.

One main motivation of this research is to develop a technique to further improve the computational efficiency and numerical stability in the wake solution as well. In order to achieve the goal, a new periodic relaxation iteration (PRI) algorithm is presented which combines the relaxation of wake collocation points with the average of velocities in terms of the finite-difference technique. The sample calculations have been performed and the robust convergence characteristics of the present scheme have been demonstrated. The present method only needs to compute the induced velocity field once for each iteration revolution, so it actually has the same good computational efficiency as the time-stepping method.

A further and important concern about the free-wake modelling is whether two different types of wake methodologies, the time-stepping method and the relaxation method, can give a unique convergence result. The previous studies on the relaxation methods did not give such comparisons, which forms another main effort of the present work. The time-stepping method has encountered convergence difficulties in hover and low-speed forward flight, however, the effects of wake will become less important in high-speed flight. As a result, a medium advance ratio, at which the time-stepping method can give a converged solution, has been chosen for the comparisons and the conclusion presented.

2. Description of the method

2.1 Governing equation of vortex filaments and periodic condition

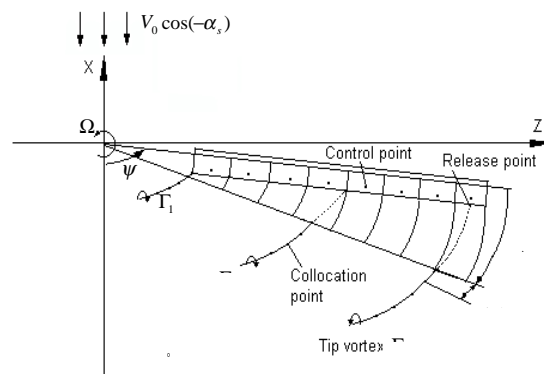


Fig. 1 Schematic of coordinate system and wake of rotor

In the present analysis, the rotor hub coordinate frame is chosen to define the wake geometry. As shown in Fig.1, the axes x and z are in rotation plane and the axis y is perpendicular to x and z , positive upward.

A vortex filament shed from blades can be described geometrically as a space curve $\vec{R}(\psi, \phi)$ in the reference system, where the ψ is the blade azimuthal angle and the ϕ is a measure of the age of the points on a vortex filament.

$$\vec{R}(\psi, \phi) = x(\psi, \phi)\vec{i} + y(\psi, \phi)\vec{j} + z(\psi, \phi)\vec{k} \quad (1)$$

According to the definition of a free wake, any of the points on vortex filaments is convected through the flowfield at the local flow velocity, so, the governing equation describing the motion of a vortex filament can be expressed as

$$\begin{aligned} \frac{d\vec{R}(\psi, \phi)}{dt} &= \Omega \left(\frac{\partial \vec{R}(\psi, \phi)}{\partial \phi} + \frac{\partial \vec{R}(\psi, \phi)}{\partial \psi} \right) \\ &= \vec{V}_0 + \vec{v}_{ind}(\vec{R}(\psi, \phi)) \end{aligned} \quad (2)$$

Where \vec{V}_0 is the free stream velocity, \vec{v}_{ind} is the induced velocity at the points of vortex filaments.

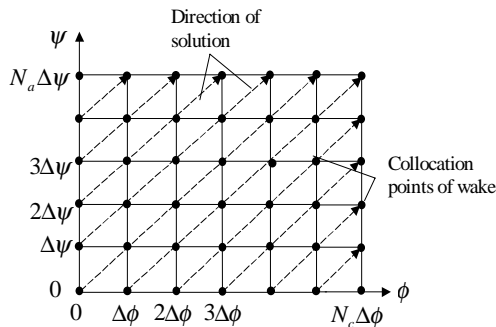


Fig. 2 Collocation points of wake

For the numerical solution of the free wake, the vortex filament is discretized as a set of collocation points and each of which is described by the variables ψ and ϕ , as shown in Fig. 2. The vortex filaments of wake in a rotor revolution are taken into account and the blade azimuthal angles and vortex filaments are discretized in the following forms, respectively

$$\psi_k = k \cdot \Delta\psi \quad k = 1, 2, \dots, N_a \quad (3)$$

Where N_a is the number of intervals for a rotor revolution.

$$\phi_j = j \cdot \Delta\phi \quad j = 1, 2, \dots, N_c \quad (4)$$

Where N_c is the number of age intervals for a vortex filament.

For the steady flight states such as hover and forward flight, the rotor wake is periodic with respect to the blade azimuth angle ψ , i.e., the wake of rotor will repeat for each separate rotor revolution. Thus, the wake collocation points for each vortex filament can be also described as

$$\vec{R}(\psi_k, \phi_j) = \vec{R}(\psi_k + 2\pi n, \phi_j) \quad n = \oplus 0, 1, \dots \quad (5)$$

Eq. (5) is known as the periodic boundary condition of wake. It should be noted that the wake collocation points satisfying the periodic condition are no longer the points defined in the conventional time-stepping methods. In the time-stepping methods, the collocation points are described in a Lagrangian sense. Over each time step, the collocation points on vortex filaments convect with the fluid at the local velocity. Typically, a new vortex segment is added onto the beginning point of wake, and in the meanwhile, an old vortex segment is discarded at the end of wake so as to keep the total number of vortex segments for each vortex filament constant. As such, the Lagrangian collocation points do not really return to the corresponding locations on the last rotor revolution, even for a converged wake, i.e., the wake described in a Lagrangian manner does not actually demonstrate the periodic feature for a steady flight condition (Ref. 13).

2.2 Wake model

Since a primary focus of this paper is the investigation of wake numerical characteristics, a non-complex free wake model is given. The rotor blade wake is characterised by a rapidly rolled-up concentrated tip vortex and the tip vortex has a dominant effect on rotor flow field. Here, the roll-up of wake is modelled and the near shed vorticity is also included in order to obtain the unsteady influence of the blade circulation and loading. As shown in Fig. 1, the rotor wake consists of the near and far components. The near wake is left undistorted and includes a set of the finite-length horseshoe trailing vortices from the blade as well as shed vorticity. The far wake is composed of one tip vortex and two inboard vortices. The tip vortex is modelled by allowing the trailed vortex portion outside of the maximum bound circulation to roll-up rapidly into a strong concentrated vortex filament

with a maximum value of blade bound circulation as its strength. The release point of the tip vortex at the trailing edge of blade is determined by calculating the centroid of vorticity, which is physically correct (Ref. 15). In some of the past wake analyses, the inboard vortex sheet is often modelled as one root vortex with the same vortex strength as the tip vortex in order for the conservation of vorticity, which has a sensitive influence on the calculation of blade circulation or induced velocity field. In the present method two discrete inboard vortex filaments are given to alleviate the influence. The release points of inboard vortex filaments have less importance than that of the tip vortex, and the two release points are chosen to be located at the first division point and a particular middle division point of blade segments for the solution of blade bound circulation, respectively, so that the sum of the bound circulation for the two filaments is equal to the maximum bound circulation. In the solution of wake, the tip vortex and two inboard vortices are free, i.e., convecting at the local velocity in the fluid.

In Fig. 1, the blade/wake junction is handled with an overlap near-wake scheme. It is a practical approach to the simulations of both the wake roll-up and the shed vorticity and has also been used in a few other rotor analyses. The main advantage of this approach is to be able to use the different number of free vortex filaments from the horseshoe trailers behind the blade and this will greatly improve computational efficiency. It has been known that a small-angular overlap near-wake region will not lead to inaccuracies in the wake solution.

2.3 Method of Solution

Eq. (2) is a partial differential equation (PDE) with the induced velocity term on the right hand side. The induced velocity term includes the self and mutually induced contributions due to the vortex filament itself and all the other vortex filaments, which is dependent on the locations of wake collocation points. It is the highly nonlinear right-side term that increases the difficulty of the numerical solution to the equation.

The finite difference method is an efficient solution to the problem. The partial differentials in the governing PDE can be approximated using different types of finite difference schemes, e.g. Refs. 13-15. In the present analysis, a five-point difference scheme with the equal difference steps in

both space (ϕ) and time (ψ) directions, i.e., $\Delta\psi = \Delta\phi$, has been chosen for the solution of free wake problem. The advantage with the equal difference steps is its convenience in comparing the calculations between the conventional time-stepping method and the relaxation method. The five-point difference scheme is considered to be superior to the simpler three-point difference scheme. Using this approach, the difference equation of Eq. (2) can be written as

$$\begin{aligned} (\bar{R}(\psi_k, \phi_j) - \bar{R}(\psi_{k-1}, \phi_{k-1})) = & \frac{\Delta\psi}{\Omega} \{\bar{V}_0 + \\ & + \frac{1}{4} [\bar{v}_{ind}(\psi_{k-1}, \phi_{j-1}) + \bar{v}_{ind}(\psi_{k-1}, \phi_j) \\ & + \bar{v}_{ind}(\psi_k, \phi_{j-1}) + \bar{v}_{ind}(\psi_k, \phi_j)] \} \end{aligned} \quad (6)$$

The initial condition for above difference equation is

$$\begin{aligned} \bar{R}(\psi, 0) = & -r_{vi} \cos \psi \cos \beta \hat{i} + r_{vi} \sin \beta \hat{j} \\ & + r_{vi} \sin \psi \cos \beta \hat{k} \end{aligned} \quad (7)$$

Where β is flapping angle and r_{vi} is blade radius where vortex filament is shed.

The boundary condition that Eq. (6) must satisfy is the periodic condition described by Eq. (5).

On the solution of the implicit difference equation with initial and boundary conditions, the present analysis gives the following scheme,

$$\begin{aligned} \bar{R}^{n+1}(\psi_k, \phi_j) = & \bar{R}^{n+1}(\psi_{k-1}, \phi_{j-1}) \\ & + \frac{\Delta\psi}{\Omega} \{\bar{V}_0 + \frac{1}{8} [\bar{v}^n(\psi_k, \phi_j) \\ & + \bar{v}^n(\psi_k, \phi_{j-1}) + \bar{v}^n(\psi_{k-1}, \phi_j) \\ & + \bar{v}^n(\psi_{k-1}, \phi_{j-1})] + \frac{1}{8} [\bar{v}^{n-1}(\psi_k, \phi_j) \\ & + \bar{v}^{n-1}(\psi_k, \phi_{j-1}) + \bar{v}^{n-1}(\psi_{k-1}, \phi_j) \\ & + \bar{v}^{n-1}(\psi_{k-1}, \phi_{j-1})] \} \end{aligned} \quad (8)$$

$$\begin{aligned} \bar{R}^{n+1}(\psi_k, \phi_j) = & \omega_R \bar{R}^{n+1}(\psi_k, \phi_j) \\ & + (1 - \omega_R) \bar{R}^n(\psi_k, \phi_j) \end{aligned} \quad (9)$$

Eq. (8) has an exception for the first iteration ($n=1$) in which the ($n-1$)th value of induced velocities is approximated by the n th one.

The present approach significantly differs from the previous pseudo-implicit predictor-corrector (PIPC) scheme developed in Ref. 15 and the simple

location relaxation scheme for time-stepping method in Ref.11, and it actually incorporates the merits of the two types of methods.

Note that the forcing term on the right side of Eq. (8) uses the average of induced velocities of the four collocation points of the current mesh (Fig. 2). Particularly, the collocation point (ψ_k, ϕ_j) to be calculated at the current step is also involved in the right-side term, which is no longer fully explicit. This average considerably helps smooth the large induced velocity perturbations occurring in wake iterations and thus effectively improve the numerical characteristics of solution. Furthermore, the induced velocities on the right side also incorporate an averaging scheme of two time-steps. Such a different time-step scheme is superior to the same time-step scheme in enhancing the numerical stability. In fact, one of the reasons causing the computational instability of wake is that the mutual induced velocity obtained from the B-S law is magnified unrealistically when two any vortex elements move very close to each other, therefore the relaxation method is considered to be particularly advantageous for the free wake problems. The physics of Eq. (9) is a weighed average of the new information and old information on calculated collocation points, and its use further improves the numerical stability and increases the converged rate.

The numerical tests have shown that the small change of the relaxation factor in Eq. (9) does not affect the converged results and its main influence is only in increasing and decreasing the number of iterations for convergence. A value of 0.6-0.8 can be suggested for calculations, typically, $\omega_r=0.7$.

The above algorithm is the periodic relaxation iteration (PRI) approach with both the average of velocities and the relaxation of collocation points, and it has used the periodic boundary condition of wake. As far as the computation time is concerned, the present scheme only needs half the computation time of the previous PIPC scheme because it does not need to compute the induced velocity field twice for each iteration revolution as done in the PIPC scheme. It is well known that the induced velocities on all the collocation points are the primary time-consuming computation in the free wake solution. Therefore, the present approach significantly improves computational efficiency when compared to the previous PIPC method, which is very important for complex rotor free wake calculation,

especially for the routine rotor analysis.

2.4 Coupling of blade aerodynamics

The second-order lifting-line theory is used to model the blade in this analysis. In comparison to the first-order lifting-line theory with the control points on the $1/4$ -chord line of blade, the second-order lifting line theory is known to be more accurate for improving the calculation of the blade-tip 3-D effects, especially for low aspect-ratio blades and close blade-vortex interaction (BVI). In the second-order lifting-line analysis, each blade is divided into a finite number of spanwise segments with a spanwise bound vortex located on the $1/4$ -chord line and a control point placed at the middle of $3/4$ -chord line in each segment. Both the spanwise and chordwise bound vortices constitute the bound vortex system of the blade, and the bound circulation is solved by satisfying the boundary condition on the control points.

The second-order lifting-line model is actually a simplified lifting-surface vortex lattice model with one chord segment. The blade aerodynamic and wake model are coupled by the solution of bound circulation. The solution of bound circulation involves the computations of the influence coefficient on each blade spanwise control point and the influence coefficient consists of the contribution of both bound vortex and wake vortices. By applying the non-penetrating boundary condition of flow on control points, a system of linear algebraic equations including the blade circulation as the unknowns can be derived and used for solving the bound circulation distribution. Usually, in the blade aerodynamic analyses using the conventional first-order lifting-line theory, the solution of blade bound circulation is carried out in an iterative matter between the induced velocity and bound circulation, which is not always stable. In the present analysis using the second-order lifting-line model, the system of linear equations can be directly solved using the standard matrix technique without the concern whether the circulation solution will converge.

Currently, the blades are assumed to be rigid and the blade flapping motion is the only degree of freedom considered. A more detailed description on the blade model can be found in Ref. 18.

In the free wake analysis, the calculations of blade circulation distribution and wake point locations are coupled to obtain a compatible

wake/circulation solution, i.e., the blade bound circulation and the wake reach converged results at the same time.

Once the blade bound circulation is known, the induced velocity at arbitrary locations in the rotor flow field and the forces on the blades can be easily calculated. When making the comparison with experimental data, a trimmed solution should be included to give a physically practical result (Ref. 16). The present analysis uses the trim method developed in a previous paper (Ref. 21). The trim method is based on the finite-difference approximations of blade flapping motion as well as trim Jacobian. It adjusts the rotor collective and cyclic pitch controls to acquire a specific thrust and flapping angles, or alternatively, the trim of adjusting the flapping angles to obtain the desired cyclic pitches can be achieved.

2.5 Convergence criteria of wake

The convergence criteria for the wake geometry is based on the change of a modified root mean square (RMS) in the wake geometry between two successive wake iterations, and the RMS is defined in the following form

$$RMS = \sqrt{\frac{\sum_k^{N_s} \sum_j^{N_c} \sum_i^{N_a} [\vec{r}_w^n(i, j, k) - \vec{r}_w^{n-1}(i, j, k)]^2}{N_s N_c N_a}} < \epsilon \quad (10)$$

Where \vec{r}_w denotes the location vector of a wake collocation point and ϵ represents the convergence threshold. The N_s is the number of the trailed vortex filaments, N_c is the number of collocation points used to describe each of trailed vortex filaments, and N_a is the number of blade azimuth steps for each rotor revolution.

For the iterative solution of rotor wake, the RMS is a proper measure of indicating convergence characteristics. The wake convergence can usually be reached after the RMS value drops below a specific threshold. The value can be easily determined by examining the wake geometry between two successive iterations. However, it should be noted that, the RMS is related to the total number of wake collocation points and the different choice of N_s, N_c and N_a will change the magnitude of RMS. So, when comparing the wake

convergence characteristics for different cases, the total number of wake collocation points should be kept to be the same in order to give a correct judgement.

3. Results and discussions

3.1 Validation of the method

The wind-tunnel experimental data on the induced velocity distribution of an isolated rotor by Georgia Tech in Ref. 19 are taken to help validate the present method first. The experimental rotor model consisted of a 2-bladed teetering rotor with NACA 0015 airfoil sections. The blades were rectangular and had no twist. The radius and chord of blades were 0.45 metres and 86 mm, respectively. In the Georgia Tech's experiments, the rotor shaft was mounted to be tilted for 6 degrees to simulate forward flight. The rotor speed was 2100 rpm and the advance ratio was 0.1. The velocity field was measured along different longitudinal lines in the rotor wake under the rotor disk plane using a Laser Doppler Velocimeter (LDV).

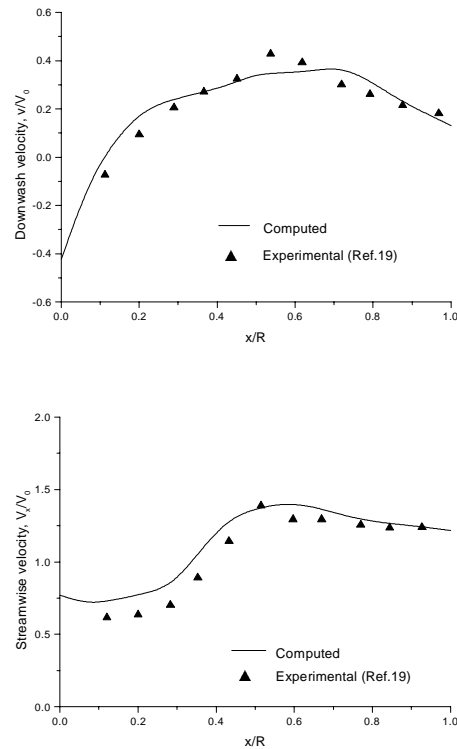


Fig. 3 Comparison of computed and experimental induced velocities

Fig. 3a and 3b show the correlation of the calculated results and experimental data in both downwash and streamwise velocity components.

The time-averaged velocity data were measured along a line one-chord length under the tip path plane (Ref. 19) and represented by the points in the figures. As indicated in Fig. 3, overall, the correlation is found to be good.

It should be pointed out that, for the teetering rotor in this case, a slightly different approach with the one used for an articulated rotor is needed when calculating the rotor trim. In contrast to an articulated rotor, the flapping motion equation of a teetering rotor is obtained by considering equilibrium of moments on the entire rotor not on one blade, as its two blades are physically connected to form a single structure.

In order to validate further the present wake model, the comparisons on the tip vortex displacements are also given here. Although considerable measurement results are available on the wake geometry of hovering rotors, experimental data on the wake geometry of forward-flight rotors, which can be used for comparison purposes, are rather less in the past. One of the reasons is that the experiments on the wake visualisation and measurements may be much more difficult in forward flight than in hover. Additionally, the wake geometry in forward flight varies very much with operational conditions and rotor parameters, especially for low-speed forward flight. Recently, however, Maryland University (Ref. 20, 14) provided a set of important experimental data on the rotor wake geometry in low-speed forward flights of $\mu = 0.05, 0.075$ and 0.1 by using a newly developed Wide-field Shadowgraph technique.

The model rotor consisted of four blades with a fully articulated hub. The rotor blades were rectangular in planform with a diameter of 1.65 metres and a chord of 6.35 mm. The linear twist of the blade is 12 degrees and the rotor was trimmed to eliminate the once-per-rev blade flapping response in the experiments.

Fig. 4a, 4b and 4c present the comparisons of the streamwise and vertical displacements of tip vortices from the aft portion of the rotor disk at the three advance ratios, respectively. As seen in Fig. 4, the fairly good agreement is achieved, with a slight exception of the region after the wake age of 200° on the vertical displacements in Fig. 2a. The cause for this discrepancy within the region is not very clear, but Ref. 15 with a different analytical method also shows the similar discrepancy.

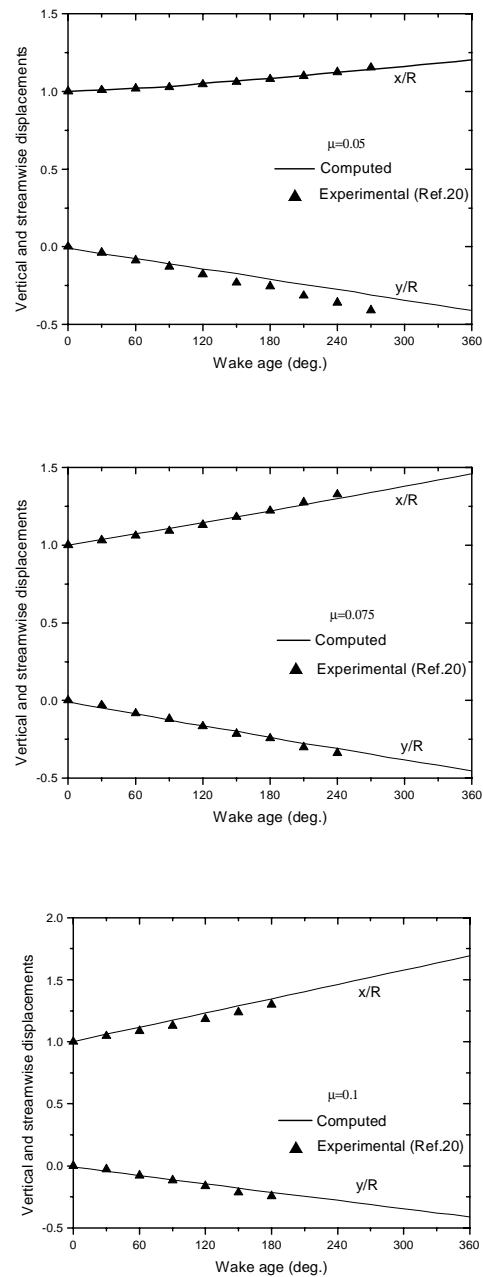
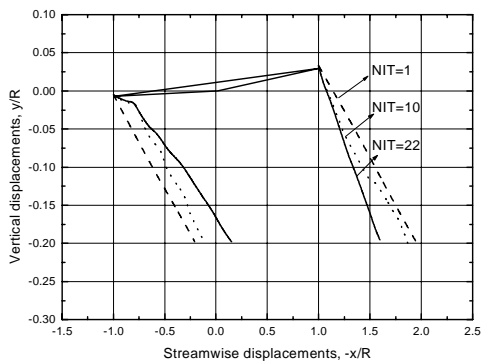


Fig. 4 Comparisons of streamwise and vertical displacements of tip vortices

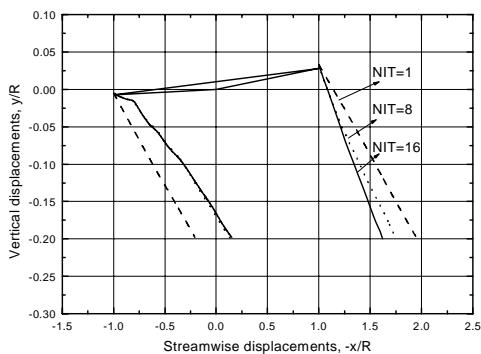
3.2 Comparison of relaxation and time-stepping methods

The free-wake solution can be generally classified as two kinds of methodologies, the time-stepping method and the non-time domain relaxation method. As stated previously, an important concern about the free-wake calculation using the non-time domain relaxation method is whether it will give an identical convergence result as the time-stepping method. The previous research on the wake

relaxation methods did not try to give such a comparison. In the present work, such a comparison has been carried out on the wake boundaries of rotor. As has been described, for hover and low-speed forward flight, the wake solution of the time-stepping method has encountered numerical instability, while in high-speed flight, the effect of wake will become less important. Therefore, a medium velocity with an advance ratio of 0.15, at which the time-stepping method can give a converged result, is chosen for comparisons.



a)The time-stepping method



b)The relaxation method

Fig. 5 Comparison of wake boundaries by relaxation and time-stepping methods

Fig. 5 shows the wake boundaries calculated by both the conventional time-stepping method and the present relaxation method. The NIT denotes the number of rotor iterations/revolutions. NIT=1 corresponds to an initial value of wake given by a rigid wake. The dotted line is a middle calculated result and the solid line represents the final converged wake boundary. Obviously, these two different types of methods can give unique converged results. Fig. 5 also demonstrates a faster convergence with the relaxation method. As noted in

Fig. 5, since the wake has a larger downward component of free stream velocity for the chosen advance ratio, the tip vortex will no longer move above the leading edge of rotor disk as in low-speed flight.

For this case, the PIPC algorithm in Ref. 15 was also investigated and the same converged wake boundary could be obtained (not shown). Additionally, numerical tests for the different cases changing the advance ratio and wake parameter were also made and the same conclusion was drawn when comparing the calculations of the present method and the time-stepping one.

3.3 Numerical characteristics of the method

To improve the numerical characteristics of wake calculations in hover and low-speed forward flight is one of the major efforts of this research. Here, the rotor of the Lynx XZ170 helicopter (Ref. 22) has been used as an example to investigate the convergence characteristics of the present method. This rotor consists of 4 rectangular blades with a hingeless hub. The radius and chord of blades are 21ft and 1.296 ft, respectively. More description on the rotor parameters can be found in Ref. 22.

Fig. 6 gives the computed RMS changes of wake geometry between two successive iterations by the present method, the PIPC method and the time-stepping method in hover and at two low advance ratios ($\mu = 0.05$ and 0.1). The RMS is defined in Eq. (10) and used to indicate the tendency of numerical characteristics. For each case of this example, the convergence of wake geometry calculated by the present and PIPC methods can be achieved after the RMS value drops below 10^{-3} , so a value of 10^{-3} can be used approximately as a threshold of convergence. In the figures, the logarithmic coordinate has been adopted to obtain a magnified view for small RMS values below 10^{-3} .

As seen in Fig. 6, the explicit time-stepping method gives a smooth variation of RMS results with the number of iterations and it does not obtain the converged solution for all three advance ratios. For both the present and PIPC methods, the convergence of wake geometry can be reached quickly for each case. The present relaxation method does exhibit strong trends of convergence and suggest the important potential in improving the difficult wake calculations for hover and low-speed

forward flight, and it is a robust algorithm. It should also be kept in mind that the present method only needs half computation time of the PIPC method because it does not need to calculate the induced velocity field twice for each iteration revolution as done in the PIPC method. It has been found that the present method actually has a nearly same computation time as the time-stepping method, so it can be easily used for the routine rotor analysis and the unsteady rotor/fuselage interactional analysis. In the calculations of the example, 3 turns of free wake and $\Delta\psi = 15^\circ$ are used.

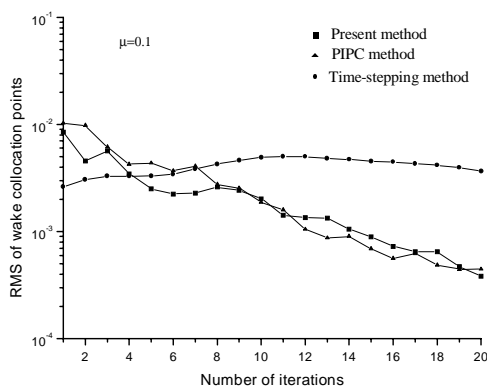
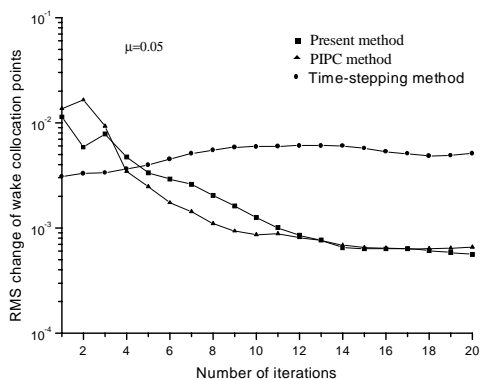
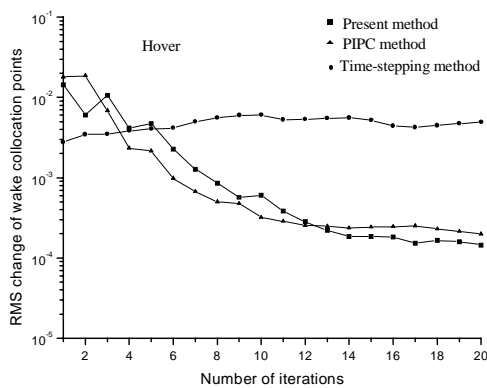


Fig. 6 Comparisons of convergence characteristics of different methods

The wake calculations on the Maryland model rotor (Ref. 19) are also performed to help validate the present method. The calculated results are showed in Fig. 7. In this case, 20 azimuth intervals of each rotor revolution and 3 turns of free wakes are chosen and the calculated advance ratio is $\mu = 0.075$. As noted in the figure, the same conclusion as in Fig. 6 can be drawn when comparing the calculations of present method, the PIPC method and the time-stepping method.

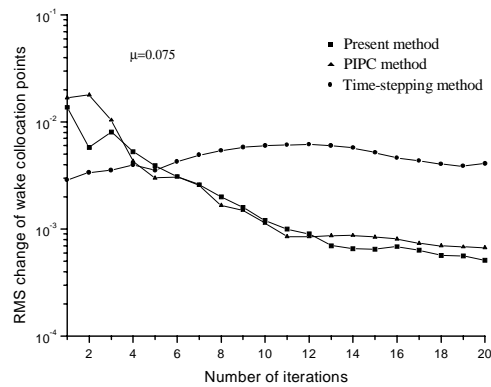


Fig. 7 Comparisons of convergence characteristics of different methods

3.4 Application of the method

The current method is applied to obtain an overview of the rotor wake structure from hover to low-speed forward flight.

Both hovering and low-speed flight are significant regimes for the rotor/fuselage or rotor/wing/fuselage interactional problems of conventional or compound helicopters. Low-speed forward flight is also the critical transition regime from the viewpoint of stability and control as well as vibration. In hovering and low-speed forward flight, the vortex wake dynamics has a more important effect than in a higher-speed flight. The conventional time-stepping methods have experienced the convergence difficulties in free-wake calculations in the regime. It is difficult to determine a boundary of this regime for different helicopters with the changing thrust levels and number of blades. However, for typical rotors, the advance ratio of 0.1 may be taken as a rough boundary value below which the numerical problems of free wake are thought to be more important (Ref. 7).

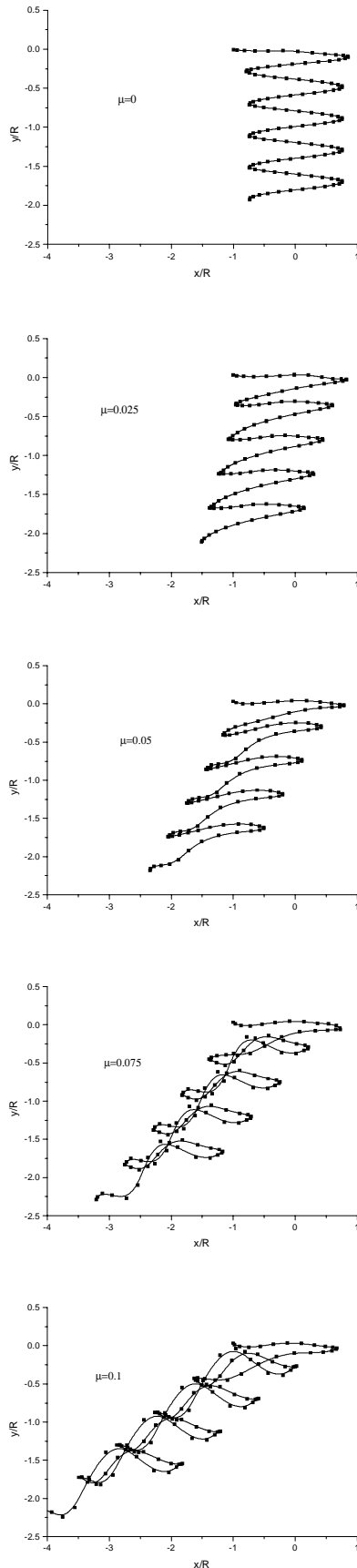


Fig. 8 Rotor wake geometry from hover through low-speed forward flight

Fig. 8 gives the calculated tip vortex geometry for 5 selected advance ratios. For clarity, only the tip vortex of one blade located at $\psi_b = 0^\circ$ is shown and the scales for two coordinate axes for each case are kept to be the same. In the calculations, 2 turns of free wake are used and a 15° azimuth step is chosen for all the advance ratios. As indicated in Fig. 8, the hovering rotor has a helical wake. For the higher forward flight velocities (0.075 and 0.1), the rotor wake demonstrates a highly distorted characteristic with an evolving roll-up along the wake edge.

At $\mu = 0.025$, the wake is approximately a skewed helix. Obviously, there is a transition at around $\mu = 0.05$, as seen in Fig. 5c, from a helical hovering wake to a highly distorted and rolled-up forward flight wake. The transition value of μ will vary with the change of the rotor thrust and wake parameters, however, Fig. 8 gives a typical feature of wake structure from hover to forward flight.

4. Conclusions

This paper presents a non-time domain relaxation algorithm using the average of velocities according to the finite-difference scheme and the relaxation of wake collocation points. A free wake analytical model based on the algorithm was given. The example calculations on the induced velocities and wake geometry were performed and the free-wake structure in transition flight conditions was analysed by applying the model. The comparisons between the two types of wake solution methodologies were carried out and the numerical characteristics of this method were investigated.

The following conclusions has been drawn from this investigation:

1) The current relaxation iteration algorithm demonstrates good convergence characteristics in hover and low-speed forward flight and the same good computational efficiency as the time-stepping algorithm. The rotor free wake analytical model incorporating this algorithm is an efficient and practical method.

2) The two different types of wake methodologies, the relaxation method and the time-stepping method can obtain the same converged result.

3) The major cause of numerical instability in the rotor free-wake calculations is due to the numerical

methods used. The different methods have different numerical characteristics and computational accuracies, which affect the stability and the converged rate of solutions.

4) For the transition flights from hover through low-speed forward flight, there is also a transfer in the wake geometry, i.e., from a symmetrical contracted helical wake to an asymmetrical, rolled-up along the wake edge and highly distorted wake.

References

1. Landgrebe, A. J., An Analytical method for Predicting Rotor Wake Geometry, J AHS, Vol. 14, No. 4, 1969, pp20-32
2. Clark, D. R. and Leiper, A. C., The Free Wake Analysis---A Method for the Prediction of Helicopter Rotor Hovering Performance, J AHS, Vol. 15, No. 1, Jan 1970, pp3-11
3. Sadle, S. G., A method for Predicting Helicopter Wake Geometry, Wake-Induced Flow and Wake Effect on Blade Airloads, Presented at the 27th Annual Forum of the AHS, May 1971
4. Egolf, T. A. and Landgreb, A. J., Helicopter Rotor Wake Geometry and Its Influence in Forward Flight, Vol. 1 ---Generalized Wake Geometry and Wake Effect on Rotor Airloads and Performance, NASA CR-3726, Oct. 1983
5. Bliss, D. B., Teske, M. E. and Quackenbush, T. R., Free Wake Calculations using Curved Vortex Elements, Presented at the International Conference on Rotorcraft Basis Research, 1985
6. Johnson, W., A General Free Wake Geometry Calculation for Wings and Rotors, Presented at the American Helicopter Society 51st Annual Forum, Texas, May 1995, pp137-153
7. Quackenbush, T. R., Boschitsch, A. H. and Wachspres, D. A., Fast Analysis Methods for Surface-Bounded Flows with Applications to Rotor Wake Modeling, Presented at the AHS 52nd Annual Forum, June 1996
8. Landgrebe, A. J., An Analytical and Experimental Investigation of Helicopter Rotor Hover Performance and Wake Geometry Characteristics, USAAMRDL TR 71-24, June 1971
9. Saberi, H and Maisel, M. D. A Free Wake Rotor Analysis Including Ground Effect, Presented at the AHS 43rd Annual Forum, May 1987
10. Lee, C. S. and He, C. J., A Free Wake/Ground Vortex Model for Rotors at Low Speed in-Ground-Effect Flight, Presented at the AHS 51st Annual Forum, 1995
11. Rosen, A and Graber A., Free Wake Model of Rotors Having Straight or Curved Blades, presented at the International Conference on Rotorcraft Basic Research, Feb. 1985
12. Quackenbush, T. R., Bliss, D. B. and Wachspres, D. A., Computational Analysis on Hover Performance using a New Free Wake Method, Presented at the Second International Conference on Rotorcraft Basic Research, Feb., 1988
13. Miller, W O and Bliss, D. B., Direct Periodic Solutions of Rotor Free Wake Calculations by Inversion of a Linear Periodic System, Proceedings of the 46th Annual Forum Helicopter Society, Washington, May 1990, pp757-769
14. Crouse, G. L., Jr. and Leishman J. G., A new Method for Improving Rotor Free-wake Convergence, AIAA 93-0872, 1993
15. Bagai A, Leishman J G. Rotor Free-wake Modeling using a Pseudo-Implicit Technique--including Comparisons with Experimental Data, J. AHS, 1995, 40(3): 29-41
16. Bagai A., Leishman J. G., Free-wake Analysis of Tandem, Tilt-Rotor and Coaxial Rotor Configurations, J. AHS, 1996
17. Bagai A, Leishman J G. and Park, J., A Free-Vortex Rotor Wake Model for Maneuvering Flight, Presented at the AHS Technical Specialists' Meeting on Rotorcraft Acoustics and Aeronautics, USA, Oct. 1997
18. Xu, G. H. and Wang, S. C., An Analytical Method for Predicting Aerodynamic Characteristics of the Rotor with a Swept Tip, Acta Aerodynamica Sinica, Vol. 17, No. 3 1999
19. Mavris, D. N., Komerath, N. M. and McMahon, H. M., Prediction of Aerodynamic Rotor-Airframe Interactions in Forward Flight, J. AHS, Oct. 1989, pp37-46
20. Leishman, J G, Bagai A. Fundamental Studies of Rotor Wakes in Low Speed Forward Flight using Wide-field Shadowgraphy, AIAA-91-3232, 1991
21. Xu, G. H., Zhao, J. G. and Newman, S. J. A Full-span Free Wake Model Using Circular-arc Curved Vortex Element and Incorporating Rotor Trim Analysis, Submitted to the Aeronautical Journal, Dec. 1999
22. Lau, B. H., Louie, A. W., et al, Performance and Rotor Loads Measurements of the Lynx XZ170 Helicopter with Rectangular Blades, NASA-TM-10400, 1993